Controlled Modulation of Electronic Properties of Graphene by Self-Assembled Monolayers on SiO_2 Substrates

Zheng Yan, Zhengzong Sun, Wei Lu, Jun Yao, Yu Zhu, and James M. Tour*

Richard E. Smalley Institute for Nanoscale Science and Technology, Department of Chemistry, Applied Physics Program through the Department of Bioengineering and Department of Mechanical Engineering and Materials Science, Rice University, 6100 Main Street, Houston, Texas, 77005

ABSTRACT In this study, with self-assembled monolayers (SAMs) of aminopropyl-, ammoniumpropyl-, butyl-, and 1*H*,1*H*,2*H*,2*H*-perfluorooctyltriethoxysilanes deposited in-between graphene and the SiO_2 substrate, a controlled doping of graphene was realized with a threshold voltage ranging from −18 to 30 V. In addition, the SAMs are covalently bonded to the SiO_2 surface rather than the graphene surface, thereby producing minimal effects on the mobility of the graphene. Finally, it is more stable than conventional noncovalent dopants.

KEYWORDS: graphene · SAMs · FET devices · threshold voltage shift

Since its first isolation in 2004, graphene, one or a few atomic layers of graphite, has attracted enormous attention for its excellent electronic properties.[1−4] In particular, its extremely high mobility and potential for use in top-down fabrication of electronic devices has made it a promising candidate for high frequency transistors.[5,6] Pristine monolayer graphene exhibits a standard ambipolar behavior with a zero neutrality point in field-effect transistors (FETs) on standard SiO_2 substrates, and the ambipolar properties limit its electronics applications. In this regard, many efforts have been made to modify the electronic structure of graphene to make n- and p-type FETs.[7−17] Present doping methods either suppress graphene's mobility or are not stable long-term.[9−17] Thereafter, for both pristine graphene and doped graphene, different methods to produce high quality, monolayer and few-layer graphene films have been disclosed.[17−19] Similar to the use of silicon in the semiconductor industry, doping and controlling the electrical structure of graphene has become important if it is to be used in place of or in addition to silicon. Direct substitution with boron and nitrogen in the graphene lattice can lead to p- and n-type doping, respectively.[14−17] However heteroatom substitutions break the symmetrical structure of the graphene lattice and lead to a 10−100-fold decrease in graphene's carrier mobilities.[14−17] Other methods include physically or chemically doping graphene with small molecules.[10−13] Physically adsorbed molecules are not stable and are easily desorbed under vacuum or heat, while chemical functionalization suppresses the mobility of graphene due to the newly formed sp^3 C−C bonds.

The transport behaviors of graphene transistors can be significantly affected by the substrates used in making the devices. It is known that graphene FET devices on SiO_2 substrates have lower carrier mobility than suspended devices or devices on boron nitride substrates.[20,21] In both cases, the research was focused on graphene's mobility. The use of self-assembled monolayers (SAMs) is a technique well-known for modification of surfaces including SiO_2.[22−31] The use of SAMs has made a significant impact on the electrical properties of organic thin film transistors (TFTs) and single-walled carbon nanotube (SWCNT) field effect transistors.[22−26] However, limited research has been done to provide controllable doping, both n-type and p-type, in graphene FET devices by functionalizing the SiO_2 substrates with SAMs.[28]

In this paper, the electrical transport behavior of graphene transistors was investigated after the modification of the SiO_2 substrates with alkyltriethoxysilane-based SAMs. The threshold voltage shift (V_{th}), which directly corresponds to the neutrality point in graphene FET devices, can be systematically controlled. Both n-type and p-type FET behaviors have been demonstrated through this technique. Additionally, the

* Address correspondence to tour@rice.edu.

Received for review December 15, 2010 and accepted January 25, 2011.

Published online February 03, 2011
10.1021/nn1034845

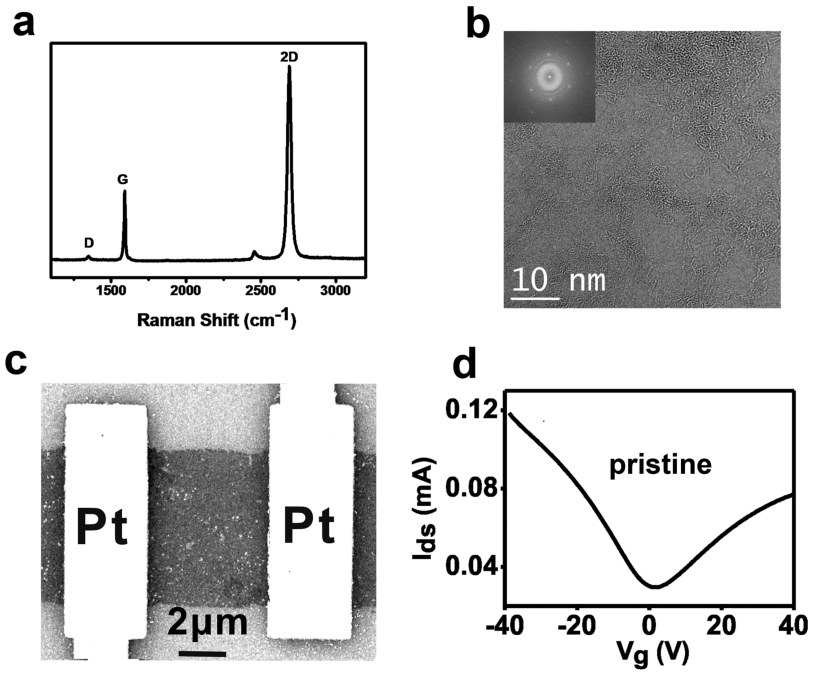

Figure 1. Characterisitics of pristine graphene. (a) Raman spectrum (laser 514 nm) of a monolayer graphene film transferred on a SiO_2/Si substrate. (b) HRTEM images of a suspended graphene film onto a TEM grid. Inset is the hexagonal FFT pattern of the image, which indicates the single-crystalline structure of the graphene. (c) SEM image of a graphene-based FET device (4 μm $\times$ 5 μm ($L \times W$)) atop a 100 nm SiO_2/Si wafer with 30 nm Pt as the source and drain electrodes. (d) The FET $I-V$ curve of pristine graphene on untreated SiO_2/Si substrate (I_{ds} = 100 mV).

SAM-induced doping has a limited impact on graphene's mobility and the SAMs remain stable even in vacuum.

The graphene film was grown using a solid carbon source: PMMA.[17] The obtained graphene was monolayer, which was confirmed by both Raman spectroscopy and high resolution transmission electron microscopy (HRTEM) (Figure1a,b). The sharp 2D peak in the Raman spectrum at 2690 cm^{-1} has a full width half-maximum (fwhm) of $\sim$30 cm^{-1} and the I_{2D}/I_G ratio is about 3, hence indicative of a typical monolayer graphene. The hexagonal fast Fourier transform (FFT) pattern for the HRTEM image suggests the graphene film is highly crystalline with few defects, a finding which correlates with the presence of the small D peak (1350 cm^{-1}) in the Raman spectrum. A highly doped Si substrate (ρ = 0.005 ohm-cm) capped with a 100 nm thick SiO_2 layer was used for the back-gated graphene FETs, and a SEM image of the as-made device is shown in Figure 1c. The source and drain electrodes (30 nm thick Pt) were defined by conventional electron-beam lithography and lift-off processes on the graphene devices. Graphene stripes (5 μm wide) were further defined by oxygen-plasma etching. Figure 1d shows the I_{ds}/V_g curve of the control sample, which exhibits a weak p-type behavior due to the unintentional doping induced by water, oxygen, or other species adsorbed from the atmosphere.

Three alkyltriethoxysilane compounds were used to prepare SAMs on the SiO_2, and four different SAM films were ultimately prepared. The alkyltriethoxylsilanes used to prepare the SAMs were: 1*H*,1*H*,2*H*,2*H*-perfluorooctyltriethoxysilane, (F-SAMs); butyltriethoxysilane, (CH_3-SAMs); 3-aminopropyltriethoxysilane (H_2N-SAMs); and the protonated form produced from the H_2N-SAMs, H_3N^+-SAMs. The detailed processes to prepare and characterize the SAMs films on SiO_2 are discussed in the Supporting Information methods and Figure 1S. In Figure 2, both XPS and water contact angle measurements support the conclusion that the SAMs were successfully prepared on SiO_2. Figure 2 panels a and b show the F1s and C1s high-resolution spectra of the F- and CH_3-SAMs, respectively, which agree well with the reported values.[27] Figure 2c displays the N1s high-resolution spectrum for the H_2N-SAMs. The N1s peak in Figure 2c can be fitted with two components centered at 399.1 (90%) and 401.5 eV (10%), which can be assigned to the free amine (H_2N-) and the ammonia cation (H_3N^+), respectively.[31] The H_3N^+-SAMs were obtained through protonation of the H_2N-SAMs with 1.0 M sulfuric acid for 24 h. The H_3N^+-SAMs XPS spectrum (Figure 2d) displays a large contribution of the ammonia cation (90%) and only a small portion of the free amine (10%). The thicknesses of the SAM films were determined by ellipsometry and the values are listed in Table 1. All four SAM films showed an average thickness $\sim$1 nm, implying a monolayer-level coverage.[22,23,27] After forming the SAMs, graphene films were transferred to the SAMs/SiO_2/Si substrates and made into FET devices (see Supporting Information for details). Figure 3 shows a schematic structure of the completed devices, where the SAM layers are

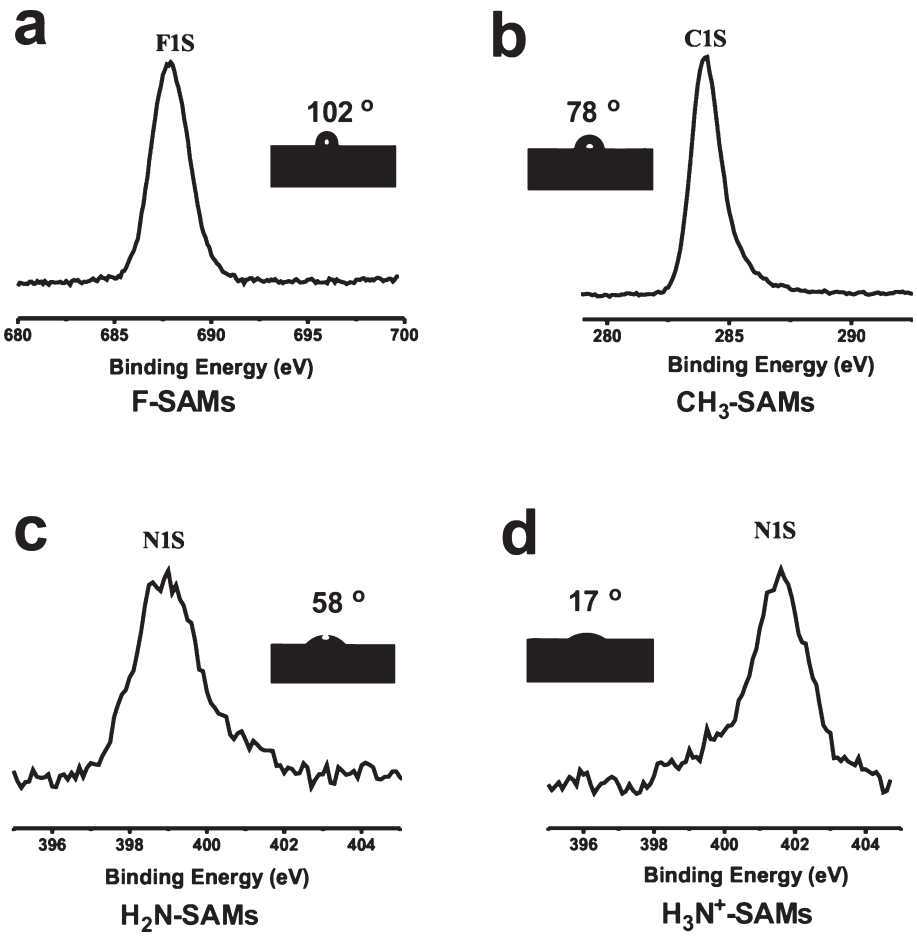

Figure 2. Characteristics of SAM films. (a) XPS analysis from the F1s peak (688 eV) and the water contact angle of F-SAMs film (102°). (b) XPS analysis of the C1s peak (284.5 eV) and the water contact angle of CH_3-SAMs film (78°). (c) XPS analysis from the N1s peak (398.8 eV) and the water contact angle of H_2N-SAMs film (58°). (d) XPS analysis of the N1s peak (401.8 eV) and the water contact angle of H_3N^+-SAMs film (17°). No F1s, C1s, or N1s peaks were observed for the untreated substrate.

in-between the graphene and SiO_2 and directly bonded to the SiO_2 substrates.

To determine the doping effects of the SAMs, the transport properties of the graphene FETs on different SAMs were measured in vacuum (Figure 4). For the graphene FET device made atop F-SAMs, the most positive V_{th} shift was observed (*ca.* +30 V, Figure 4a), while only *ca.* −8 V V_{th} shift (Figure 4b) was observed for the device made on CH_3-SAMs, indicating that butyl groups lead to a weak n-doping effect in the graphene FET devices. For the device fabricated on H_2N-SAMs, the V_{th} is downshifted to *ca.* −18 V (Figure 4c), suggesting that aminopropyl SAMs have a relative strong n-doping in the graphene FET device. Compared to H_2N-SAMs, the opposite doping effect is shown in Figure 4d on H_3N^+-SAMs supported devices, with a V_{th} upshifted to *ca.* +20 V. With the four different SAMs, a wide range of V_{th} values have been obtained, from −18 V (H_2N-SAMs, n-doping) to +30 V (F-SAMs, p-doping). For each SAM film, more than five devices were fabricated and similar results were observed for each set (standard deviation, <3).

TABLE 1. Summary of Characterization Data on SAMs in the Study

	end group	CF_3	CH_3	H_2N	H_3N^+
SAMs thickness (Å)	present results	11.1	6.2	10	11
	calculated results	10.6[27]	5.3[23]	5.5[22]	n/a
water contact angle (deg)	present results	102	78	58	17
	reported results	105[27]	75[23]	60[29]	n/a

The observed systematic doping can be explained by built-in electric dipoles and the charge transfer between SAMs and the graphene channels. The dipole alignment of the SAM molecules is thought to produce a built-in electric field and thereby modify the carrier density of organic field-effect transistors.[22,24] The theoretical model works well in explaining CH_3- and F-SAMs induced doping in graphene transistors. The dipoles of molecules similar to F-SAMs and CH_3-SAMs have been calculated by Kobayashi *et al.* using density function theory (DFT).[22] The dipole moments along the molecular axes were computed as −2.202 and 0.831 D for F-SAM and CH_3-SAM, respectively. The built-in electric field inside the SAMs can be estimated by $E = N(\mu/d\varepsilon\varepsilon_0)$,[22,32] where N is the molecular density, d is the

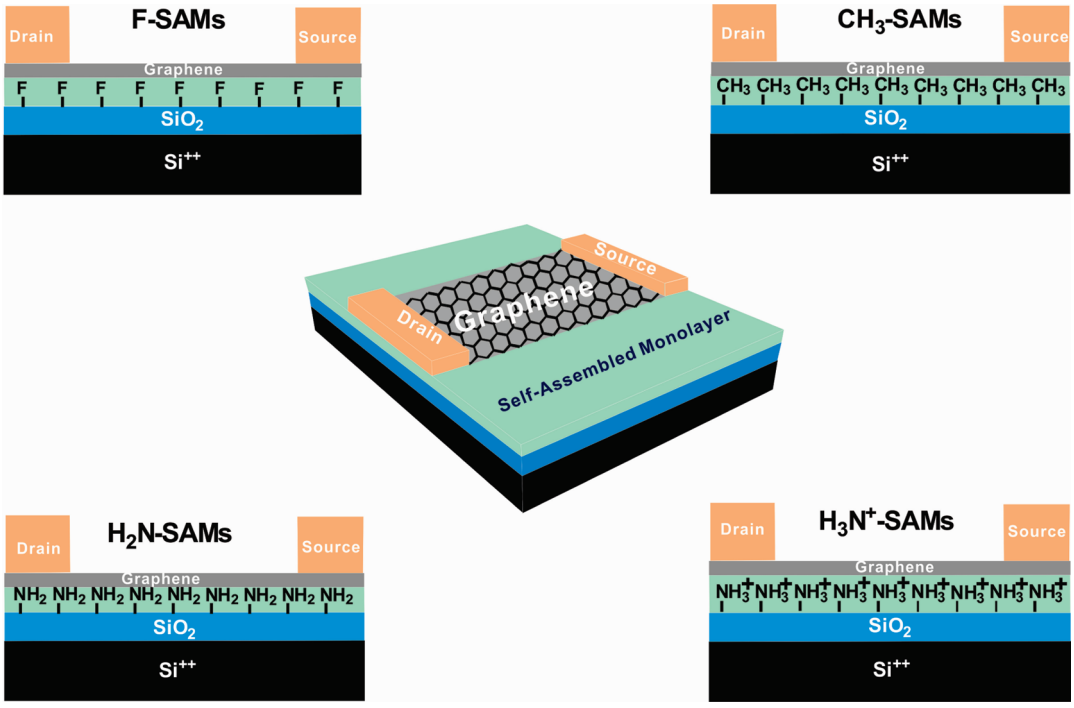

Figure 3. Schematic diagram of the graphene FET devices fabricated in this study.

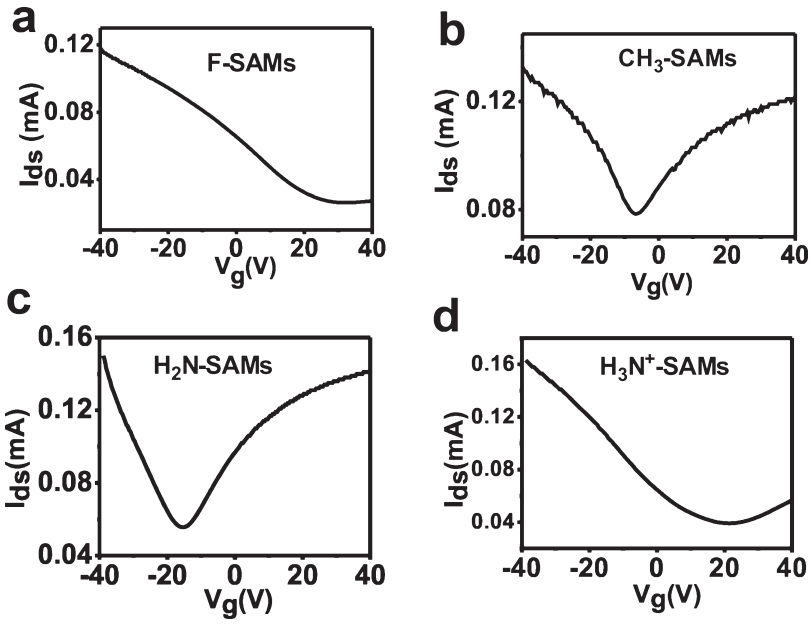

Figure 4. I_{ds}/V_g characteristics of graphene based FET devices on different SAMs. Room temperature $I_{ds}-V_g$ curves of the FET devices fabricated on (a) F-SAMs, (b) CH_3-SAMs, (c) H_2N-SAMs, and (d) H_3N^+-SAMs at V_{ds} = 100 mV.

length of the SAM molecule, ε is the effective dielectric constant inside the SAM molecules, and ε_0 is the permittivity of free space. For the SAMs in this study, N is about $1-2 \times 10^{14}$ cm^{-2}, $d_{F\text{-}SAMs}$ is 1.1 nm, $d_{CH3\text{-}SAMs}$ is 0.6 nm, and ε is between 2 and 3.[22] According to the above formula, the calculated electric fields inside the SAMs are $E_{F\text{-}SAMs} = -(2.5$ to $7.4)$ MV/cm and $E_{CH3\text{-}SAMs} = 0.94$ to 2.8 MV/cm. To produce the same electric field by applying a voltage across the 100-nm-thick SiO_2 gate insulator, a gate voltage of 25—74 V for F-SAMs and $-(9.4$ to $28)$ V for CH_3-SAMs is necessary, which agrees well with the shifts in electrical transport characteristics observed in our devices (Table 2).

However, since the amine group bears a lone pair of electrons and the ammonium group is positive charged, H_2N-SAMs and H_3N^+-SAMs induced doping in graphene transistors cannot be understood simply by using the built-in electric field model. Dai *et al.* have discussed the possible charge transfer mechanism between carbon nanotubes and aminopropyltriethoxysilane or

TABLE 2. Threshold Voltage V_{th} and Field-Effect Mobility μ Determined in the Study

end group	H_2N	CH_3	untreated	H_3N^+	CF_3
V_{th} (V)	−18	−8	4	20	30
μ ($cm^2\ V^{-1}\ s^{-1}$)	661	460	449	363	450

polyethylene imine molecules, suggesting that the electron-donating ability of the amine groups led to the efficient n-doping in carbon nanotubes.[35,36] A charge transfer mechanism, arising from the position of the highest occupied molecular orbital (HOMO) and lowest unoccupied molecular orbital (LUMO) of the molecule with respect to the Dirac-point of graphene and orbital hybridization, was also proposed to explain small molecule-induced doping.[33] The amine group in H_2N-SAMs can donate its lone pair to graphene's channel, increasing electron carrier density and inducing n-doping. In H_3N^+-SAMs, the lone pairs are occupied by H^+. The ammonium cations in H_3N^+-SAMs are positively charged, which is anticipated to withdraw electrons from the graphene channel, decreasing electron carrier density and inducing hole doping.

To define the impact of the SAMs on graphene's mobility, field-effect mobilities were extracted from the I_{ds}/V_g curves using the following formula: $\mu = [(\Delta I_{ds}/V_{ds})(L/W)]/C_{ox}\Delta V_g$.[34] Here, L and W are the length and the width of the graphene channel, respectively. And C_{ox} is calculated by $\varepsilon_0\varepsilon_r A/d$, where d is the thickness of SiO_2, A is unit area, ε_0 is the permittivity of free space, and ε_r is 3.0 for PVD SiO_2 without annealing.[34] The calculated data are summarized in Table 2. Of particular interest, the carrier mobilities of transistors on SAMs are of the same order of magnitude as transistors fabricated on untreated SiO_2 substrates. The small variances in the mobilities of these five transistors come from both the different quality of graphene due to the domain size[37] and the different SAMs. SAM doping arises from electric dipoles and charge transfer which do not introduce more scattering centers into the graphene lattice than into the bare SiO_2 substrates, therefore having limited effects on the mobilities. In addition, unlike small molecule doping that is caused by physisorption on the graphene plane,[10−13] SAMs are covalently attached to the SiO_2 surface and cannot be cleaved even in vacuum. Two SAM doping cases, H_2N-SAMs and F-SAMs were tested under vacuum (see Supporting Figure S3). After keeping the samples under vacuum (10^{-6} Torr) for 7 d, only a small positive threshold voltage shift was observed in comparison with that obtained after keeping the samples under vacuum (10^{-6} Torr) for 3 d, which was attributed to the desorption of species adsorbed from the atmosphere, including oxygen and water.[17]

In conclusion, producing stable doping and high mobility is a problem for graphene-based electronics. For such an electrically sensitive material, modulating electrical characteristics of the substrate controls the electrical characteristics of the device. By adapting the SAM techniques, systematic modulation of graphene's electronic properties becomes available without affecting its mobility. A wide doping range has been achieved with hundreds of SAMs hitherto unexplored. This technique provides a simple solution for the development of more controllable graphene devices.

EXPERIMENTAL SUMMARY

Raman spectroscopy was performed with a Renishaw Raman microscope using 514 nm laser at ambient temperature. The electrical properties were measured in a probe station (Desert Cryogenic TT-probe 6 system) under vacuum (10^{-5}−10^{-6} Torr) at room temperature. The I−V data were collected by an Agilent 4155C semiconductor parameter analyzer. The HRTEM images were taken using a 2100F field emission gun transmission electron microscope with graphene samples directly transferred on a C-flat TEM grid (Protochips, Inc.). XPS was performed on a PHI Quantera SXM scanning X-ray microprobe with 45° takeoff angle and a 100 μm beam size. The thickness of SAMs was determined by an LSE Stokes ellipsometer with a He−Ne laser light source at a λ of 632.8 nm of an angle of incidence of 70°.

Acknowledgment. We thank the AFOSR (FA9550-09-1-0581), the AFOSR through an STTR with PrivaTran, Inc., and the ONR MURI program (No. 00006766).

Supporting Information Available: Detailed experimental procedures, I−V curves, and Raman and XPS spectra. This material is available free of charge *via* the Internet at http://pubs.acs.org.

REFERENCES AND NOTES

1. Novoselov, K. S.; Geim, A. K.; Morozov, S. V.; Jiang, D.; Zhang, Y.; Dubonos, S. V.; Grigorieva, I. V.; Firsov, A. A. Electric Field Effect in Atomically Thin Carbon Films. *Science* **2004,** *306*, 666–669.
2. Geim, A. K.; Novoselov, K. S. The Rise of Graphene. *Nat. Mater.* **2007,** *3*, 183–191.
3. Novoselov, K. S.; Geim, A. K.; Morozov, S. V.; Jiang, D.; Katsnelson, M. I.; Grigorieva, I. V.; Dubonos, S. V.; Firsov, A. A. Two-dimensional Gas of Massless Dirac Fermions in Graphene. *Nature* **2005,** *438*, 197–200.
4. Ruoff, R. S. Graphene: Calling All Chemists. *Nat. Nanotechnol.* **2008,** *3*, 10–11.
5. Lin, Y. M.; Dimitrakopoulos, C.; Jenkins, K. A.; Farmer, D. B.; Chiu, H. Y.; Grill, A.; Avouris, P. 100-GHz Transistors From Wafer-Scale Epitaxial Graphene. *Science* **2010,** *327*, 662.
6. Liang, X.; Jung, Y.; Wu, S.; Ismach, A.; Olynick, D.; Cabrini, S.; Bokor, J. Formation of Bandgap and Subbands in Graphene Nanomeshes with Sub-10nm Ribbon Width Fabricated *via* Nanoimprint Lithography. *Nano Lett.* **2010,** *10*, 2454–2460.
7. Wang, X.; Li, X.; Zhang, L.; Yoon, Y.; Weber, W.; Wang, H.; Guo, J.; Dai, H. N-doping of Graphene through Electrothermal Reactions with Ammonia. *Science* **2009,** *324*, 768–771.
8. Li, X.; Wang, H.; Robinson, J.; Sanchez, H.; Diankov, G; Dai, H. Simultaneous Nitrogen Doping and Reduction of Graphene Oxide. *J. Am. Chem. Soc.* **2009,** *131*, 15939–15944.
9. Farmer, D. B.; Golizadeh-Mojarad, R.; Perebeinos, V.; Lin, Y.; Tulevski, G.; Tsang, J.; Avouris, P. Chemical Doping and

Electron-Hole Conduction Asymmetry in Graphene Devices. *Nano Lett.* **2009,** *9*, 388–392.
10. Das, B.; Voggu, R.; Rout, C.; Rao, C. N. R. Changes in the Electronic Structure and Properties of Graphene Induced by Molecular Charge-Transfer. *Chem. Commun.* **2008,** 5155–5157.
11. Gierz., I.; Riedl, C.; Starke, U.; Ast, C.; Kern, K. Atomic Hole Doping of Graphene. *Nano Lett.* **2008,** *8*, 4603–4607.
12. Chen, J. H.; Jang, C.; Adam, S.; Fuhrer, M. S.; Williams, E. D.; Ishigami, M. Charged-Impurity Scattering in Graphene. *Nat. Phys.* **2008,** *4*, 377–381.
13. Dong, X.; Fu, D.; Fang, W.; Shi, Y.; Chen, P.; Li, L. Doping Single-Layer Graphene with Aromatic Molecules. *Small.* **2009,** *5*, 1422–1426.
14. Guo, B.; Liu, Q; Chen, E.; Zhu, H.; Fang, L.; Gong, J. Controllable N-Doping of Graphene. *Nano Lett.* **2010,** *10*, 4975–4980.
15. Wei, D.; Liu, Y.; Wang, Y.; Zhang, H.; Huang, L.; Yu, G. Synthesis of N-Doped Graphene by Chemical Vapor Deposition and Its Electrical Properties. *Nano Lett.* **2009,** *9*, 1752–1758.
16. Panchakarla., L. S.; Subrahmanyam, K. S.; Saha, S. K.; Govindaraj, A.; Krishnamurthy, H. R.; Waghmare, U. V.; Rao, C. N. R. Synthesis, Structure, and Properties of Boron- and Nitrogen- Doped Graphene. *Adv. Mater.* **2009,** *21*, 4726–4730.
17. Sun, Z.; Yan, Z.; Yao, J.; Beitler, E.; Zhu, Y.; Tour, J. Growth of Graphene From Solid Carbon Sources. *Nature* **2010,** *468*, 549–552.
18. Li, X.; Cai, W.; An, J.; Kim, S.; Nah, J.; Yang, D.; Piner, R.; Velamakanni, A.; Jung, I.; Tutuc, E.; Banerjee, S.; Colombo, L.; Ruoff, R. Large-Area Synthesis of High-Quality and Uniform Graphene Films on Copper Foils. *Science* **2009,** *324*, 1312–1314.
19. Kim, K. S.; Zhao, Y.; Jang, H.; Lee, S.; Kim, J.; Kim, K.; Ahn, J.; Kim, P.; Choi, J.; Hong, B. Large-Scale Pattern Growth of Graphene Films for Stretchable Transparent Electrodes. *Nature* **2009,** *45*, 706–710.
20. Dean, C. R.; Young, A. F.; Meric, I.; Lee, C.; Wang, L.; Sorgenfrei, S.; Watanabe, K.; Taniguchi, T.; Kim, P.; Shepard, K. L.; Hone, J. Boron Nitride Substrates for High-Quality Graphene Electronics. *Nat. Nanotechnol.* **2010,** *5*, 722–726.
21. Du, X.; Skachko, I.; Barker, A.; Andrei, B. Approaching Ballistic Transport in Suspended Graphene. *Nat. Nanotechnol.* **2008,** *3*, 491–495.
22. Kobayashi, S.; Nishikawa, T.; Takenobu, T.; Mori, S.; Shimoda, T.; Mitani, T.; Shimotani, H.; Yoshimoto, N.; Ogawa, S.; Iwasa, Y. Control of Carrier Density by Self-Assembled Monolayers in Organic Field-Effect Transistors. *Nat. Mater.* **2004,** *3*, 317–322.
23. Ito, Y.; Virkar, A.; Mannsfeld, S.; Oh, J.; Toney, M.; Locklin, J.; Bao, Z. Crystalline Ultrasmooth Self-Assembled Monolayers of Alkylsilanes for Organic-Field-Effect Transistors. *J. Am. Chem. Soc.* **2009,** *131*, 9396–9404.
24. Pernstich., K. P.; Haas, S.; Oberhoff, D.; Goldmann, C.; Gundlach, D. J.; Batlogg, B.; Schitter, G. Threshold Voltage Shift in Organic Field Effect Transistors by Dipole Monolayers on the Gate Insulator. *J. Appl. Phys.* **2004,** *96*, 6431–6438.
25. Possanner, S. K.; Karin, Z.; Peter, P.; Egbert, Z.; Ferdinand, S. Threshold Voltage Shifts in Organic Thin-Film Transistors Due to Self-Assembled Monolayers at the Dielectric Surface. *Adv. Funct. Mater.* **2009,** *19*, 958–967.
26. Vosgueritchian., M.; Lemieux, M.; Dodge, D.; Bao, Z. Effect of Surface Chemistry on Electronic Properties of Carbon Nanotube Network Thin Film Transistors. *ACS Nano* **2010,** *4*, 6137–6145.
27. Hozumi, A.; Ushiyama, K.; Sugimura, H.; Takai, O. Fluoroalkylsilane Monolayers Formed by Chemical Vapor Surface Modification on Hydroxylated Oxide Surfaces. *Langmuir* **1999,** *15*, 7600–7604.
28. Wang, R.; Wang, S.; Zhang, D.; Li, Z.; Fang, Y.; Qiu, X. Control of Carrier Type and Density in Exfoliated Graphene by Interface. *ACS Nano*, published on the Web December 6, 2010; DOI: 10.1021/nn102236x.
29. Hozumi, A.; Yokogawa, Y.; Kameyama, T.; Sugimura, H.; Hayashi, K.; Shirayama, K.; Takai, O. Amino-Terminated Self-Assembled Monolayer on a SiO_2 Surface Formed by Chemical Vapor Deposition. *J. Vac. Sci. Technol. A* **2001,** *19*, 1812–1816.
30. Howarter, J. A.; Youngblood, J. Optimization of Silica Silanization by 3-Aminopropyltriethoxysilane. *Langmuir* **2006,** *22*, 11142–11147.
31. Lee, S.; Lin, W.; Kuo, C.; Karakachian, M.; Lin, Y.; Yu, B.; Shyue, J. Photo-oxidation of Amine-Terminated Self-Assembled Monolayers on Gold. *J. Phys. Chem. C* **2010,** *114*, 10512–10519.
32. Gonen, A.; Cahen, D.; Cohen, R.; Shanzer, A.; Vilan, A. Molecular Engineering of Semiconductor Surfaces and Devices. *Acc. Chem. Res.* **2002,** *35*, 121–128.
33. Rao, C. N. R.; Sood, A. k.; Subrahmanyam, K. S.; Govindaraj, A. Graphene: The New Two-Dimensional Nanomaterial. *Angew. Chem., Int. Ed.* **2009,** *48*, 7752–7777.
34. Wu, Y. Q.; Ye, P. D.; Capano, M. A.; Xuan, Y.; Sui, Y.; Qi, M.; Copper, J. A.; Shen, T.; Pandey, D.; Prakash, G..;; *et al.* Top-Gated Graphene Field-Effect-Transistors Formed by Decomposition of SiC. *Appl. Phys. Lett.* **2008,** *92*, 092102.
35. Shim, M.; Javey, A.; Kam, N; Dai, H. Polymer Functionalization for Air-Stable N-Type Carbon Nanotube Field-Effect Transistors. *J. Am. Chem. Soc.* **2001,** *123*, 11512–11513.
36. Kong, J.; Dai, H. Full and Modulated Chemical Gating of Individual Carbon Nanotubes by Organic Amine Compounds. *J. Phys. Chem.* **2001,** *105*, 2890–2893.
37. Li, X.; Magnuson, C.; Venugopal, A.; An, J.; Suk, J.; Han, B.; Borysiak, M.; Cai, W.; Velamakanni, A.; Zhu, Y..;; *et al.* Graphene Films with Large Domain Size by a Two-Step Chemical Vapor Deposition Process. *Nano Lett.* **2010,** *10*, 4328–4334.